

Linear system parameter as an indicator for structural diagnosis of short span bridges

Chul-Woo Kim^{*1}, Ryo Isemoto¹, Kunitomo Sugiura¹ and Mitsuo Kawatani²

¹Department of Civil and Earth Resources Engineering, Graduate School of Eng.,
Kyoto University, Kyoto, Japan

²Department of Civil Engineering, Graduate School of Eng., Kobe University, Kobe, Japan

(Received November 29, 2011, Revised September 27, 2012, Accepted November 30, 2012)

Abstract. This paper intended to investigate the feasibility of bridge health monitoring using a linear system parameter of a time series model identified from traffic-induced vibrations of bridges through a laboratory moving vehicle experiment on scaled model bridges. This study considered the system parameter of the bridge-vehicle interactive system rather than modal ones because signals obtained under a moving vehicle are not the responses of the bridge itself but those of the interactive system. To overcome the shortcomings of modal parameter-based bridge diagnosis using a time series model, this study considered coefficients of Autoregressive model (AR coefficients) as an early indicator of anomaly of bridges. This study also investigated sensitivity of AR coefficients in detecting anomaly of bridges. Observations demonstrated effectiveness of using AR coefficients as an early indicator for anomaly of bridges.

Keywords: AR coefficient; linear system model; health monitoring; bridge-vehicle interactive system; structural diagnosis

1. Introduction

Maintaining and improving civil infrastructure including bridge structures are important technical issues especially for industrialized nations. Moreover effective maintenance strategy strongly depends on timely decision on the health condition of the structure. Structure health monitoring using vibration data is one of promising technologies for a decision making on the maintenance. Most precedent studies on structural health monitoring specifically examine the change of modal properties and quantities of structures (e.g., Doebling *et al.* 1996). The fundamental concept of this technology is that modal parameters are functions of a structure's physical properties. Therefore, a change in physical properties, such as reduced stiffness resulting from damage, will detectably change these modal properties (Friswell and Mottershead 1994, Peeters *et al.* 2001, Deraemaeker *et al.* 2007, Zhang 2007, Dilena *et al.* 2011).

An important problem that must be solved in bridge health monitoring (BHM) using vibration measurements is how excite the bridge economically, reliably and rapidly. Ambient vibrations induced by traffic and wind are adopted as dynamic data for BHM. Especially for small and

*Corresponding author, Professor, E-mail: kim.chulwoo.5u@kyoto-u.ac.jp

medium span bridges which are majority portions of the bridge infrastructure, however, the wind is usually too weak to actuate the bridges. On the other hand, the traffic-induced vibration becomes very dominant for those small and medium span bridges. However when we consider the traffic-induced vibration of bridges in BHM, we should keep in mind that the traffic-induced vibration of bridges is a kind of non-stationary vibration (Kim *et al.* 2005, Kim and Kawatani 2008).

Many studies focus on changes of system frequencies and structural damping constants for bridge diagnosis, which are estimated utilizing a linear time-series model (e.g., Kim *et al.* 2010). Since 1970s, the use of state-space models for modal parameter identification in time-domain has been increasing and also has yielded new approaches. Gersch *et al.* (1973), for example, used the time series of an autoregressive moving average (ARMA) process to describe the random response of a vibrating structure to a white noise excitation. Shinozuka *et al.* (1982) obtain a second-order ARMA model to represent a vibrating structure in order to identify the structural parameters directly. Hoshiya and Saito (1984) include the parameters to be identified as additional state variables in the state vector using extended Kalman filter. These approaches regard the ambient vibration responses as random process of ARMA. Estimating the coefficients of ARMA model is a kind of nonlinear approach because both of the coefficients relating to AR and MA processes are unknown variables. Fortunately, the AR model with an infinite order is equivalent to the ARMA model, which means that one can express the responses of a linear system subjected to white-noise input using the AR model with sufficient large order (Wang and Fang 1986, He and De Roeck 1997).

Drawbacks of modal parameter-based bridge diagnosis using time series model is the driving force for this study: the optimal time series model for vibration responses of bridge structures usually comprises a higher order term, and as a result the optimal model detects even numerical parameters which cause false system frequencies and damping constants. Actually these false system parameters make it difficult to choose the modal parameter affected by structural damage.

Therefore an alternative parameter from AR coefficients was considered for the vibration-based BHM in this study, since both system frequency and damping constant depend on AR coefficients (Nair *et al.* 2006, Kim *et al.* 2010). Both singlevariate autoregressive (SAR) and multivariate autoregressive (MAR) models were considered.

2. SAR model and modal identification

If $\mathbf{y}_c(t)$ denotes output of a bridge structure taken from an observation point, then the corresponding state equation of a continuous-time system is described as

$$\dot{\mathbf{x}}_c(t) = \mathbf{A}_c \mathbf{x}_c(t) + \mathbf{B}_c \mathbf{f}_c(t), \quad \mathbf{y}_c(t) = \mathbf{C}_c \mathbf{x}_c(t) \quad (1)$$

where

$$\mathbf{x}_c(t) = \begin{bmatrix} z(t) \\ \dot{z}(t) \end{bmatrix} \quad (2)$$

$$\mathbf{A}_c = \begin{bmatrix} 0 & 1 \\ -k_b/m_b & -c_b/m_b \end{bmatrix} \quad (3)$$

$$\mathbf{B}_c = \begin{bmatrix} 0 \\ -1/m_b \end{bmatrix} \quad (4)$$

$$\mathbf{C}_c = [1 \ 0] \quad (5)$$

Therein, m_b , k_b , c_b , respectively indicate the mass, damping, and stiffness of a bridge. $z(t)$ denotes the displacement response, and $f(t)$ represents an external force vector. If the observability matrix is defined as $\mathbf{L}^T = [C; CA_c; \dots; CA_c^{n-1}]$, then the discrete state equation for the system from the equation of motion for a bridge through an observability transformation can be described (Ljung 1999) as

$$\mathbf{x}(k+1) = \mathbf{A}\mathbf{x}(k) + \mathbf{B}f(k) \quad (6)$$

$$\mathbf{y}(k) = \mathbf{C}\mathbf{x}(k) \quad (7)$$

where $\mathbf{x}(k) = \mathbf{L}\mathbf{x}_d(k)$, and the subscript d indicates discretized one from the continuous system. The state transition matrix \mathbf{A} , input influence matrix \mathbf{B} and output influence matrix \mathbf{C} through an observability transformation are described as

$$\mathbf{A} = \mathbf{L}\mathbf{A}_d\mathbf{L}^{-1} = \begin{bmatrix} 0 & 1 & 0 & \dots & 0 \\ 0 & 0 & 1 & & 0 \\ \vdots & & & \ddots & \vdots \\ 0 & 0 & 0 & & 1 \\ -a_n & -a_{n-1} & -a_{n-2} & \dots & -a_1 \end{bmatrix} \quad (8)$$

$$\mathbf{B} = \mathbf{L}\mathbf{B}_d = [b_1; \dots; b_n] \quad (9)$$

$$\mathbf{C} = \mathbf{C}_d\mathbf{L}^{-1} = [1 \ 0 \ \dots \ 0] \quad (10)$$

where $\mathbf{A}_d = e^{\mathbf{A}_c\Delta}$; and Δ represents the sampling period.

If coefficients from a_1 to a_n of the system matrix \mathbf{A} is known, then eigenvalues of the matrix \mathbf{A} provide the modal information of the system. Therefore, the next step is to derive linear equations for the coefficient using the measurements (or observation) $\mathbf{y}(k)$. The state equation in Eq.(6) is rewritable as

$$\begin{aligned} x_1(k+1) &= x_2(k) + b_1 f(k) \\ &\vdots \\ x_{n-1}(k+1) &= x_n(k) + b_{n-1} f(k) \\ x_n(k+1) &= -a_n x_1(k) - a_{n-1} x_2(k) - \dots - a_1 x_n(k) + b_n f(k) \end{aligned} \quad (11)$$

Using the observability equation of Eq. (7), Eq. (11) can be rearranged as

$$\begin{aligned} y(k) &= x_1(k) \\ y(k+1) &= x_1(k+1) = x_2(k) + b_1 f(k) \\ &\vdots \\ y(k+n-1) &= x_1(k+n-1) = x_{n-1}(k+1) + b_{n-2} f(k+1) + \dots + b_1 f(k+n-2) \\ &= x_n(k) + b_{n-1} f(k) + \dots + b_1 f(k+n-2) \end{aligned} \quad (12)$$

$\mathbf{x}(t)$ of Eq.(12) is rewritable as

$$\mathbf{x}(k) = \mathbf{y}(k) - \mathbf{b}f(k) \quad (13)$$

where

$$\mathbf{x}(k) = [x_n(k); x_{n-1}(k); \dots; x_1(k)] \quad (14)$$

$$\mathbf{y}(k) = [y(k+n-1); \dots; y(k+1); y(k)] \quad (15)$$

$$\mathbf{f}(k) = [f(k+n-1); \dots; f(k+1); f(k)] \quad (16)$$

$$\mathbf{b} = [\bar{\mathbf{b}}_n; \dots; \bar{\mathbf{b}}_1] \quad (\bar{\mathbf{b}}_n = \{0 \quad b_1 \quad \dots \quad b_{n-1}\}; \dots; \bar{\mathbf{b}}_1 = \{0 \quad \dots \quad 0\}) \quad (17)$$

The last relation in Eq.(11) gives

$$x_n(k+1) = -\mathbf{a}\mathbf{x}(k) + b_n f(k) \quad (18)$$

where $\mathbf{a} = \{a_1 \dots a_n\}$.

Moreover the following relation is obtainable from Eq. (12)

$$x_n(k+1) = y(k+n) - \sum_{i=1}^{n-1} b_i f(k+n-i) \quad (19)$$

Substituting Eqs. (19) and (13) into Eq. (18), and assuming $\mathbf{f}(k)$ as a white noise input $\mathbf{e}(k)$ gives the following ARMA model.

$$\mathbf{y}(k) = -\mathbf{a}\mathbf{y}(k-n) + \tilde{\mathbf{b}}\mathbf{e}(k-n) \quad (20)$$

where

$$\tilde{\mathbf{b}} = [b_1 \quad \dots \quad b_n] \begin{bmatrix} 1 & a_1 & \dots & \dots & a_{n-1} \\ 0 & 1 & a_1 & \dots & a_{n-2} \\ & & \ddots & & \vdots \\ & & & 1 & a_1 \\ & & & & 1 \end{bmatrix} \quad (21)$$

The AR model with infinite order is equivalent to the ARMA model, which means that one can express the responses of a linear system subjected to white-noise input using the AR model with sufficient large order.

$$y(k) + \sum_{i=1}^p a_i y(k-i) = e(k) \quad (22)$$

To estimate the AR parameter, the autocorrelation function of $y(k)$ is used, which is obtainable by multiplying each term of Eq. (22) with $y(k-s)$ and taking mathematical expectation. This process yields the following Yule-Walker equation

$$\mathbf{R}\mathbf{a} = -\mathbf{r} \quad (23)$$

where \mathbf{R} is a Toeplitz matrix about $R(p, s) = E[y(k-p)y(k-s)]$ which is the autocorrelation function of the signal, and $\mathbf{r}^T = [R_1; \dots; R_n]$. The Levinson-Durbin algorithm is adopted to solve Eq. (23). It is noteworthy that the coefficient a_p is a pole of the system because the z -transformation of Eq. (22) is

$$y(k) = H(z)e(k) = \frac{1}{1 + \sum_{i=1}^p a_i z^{-i}} e(k) \quad (24)$$

where $H(z)$ is the transfer function of the system in the discrete-time complex domain, and z^{-i} denotes a forward shift operator.

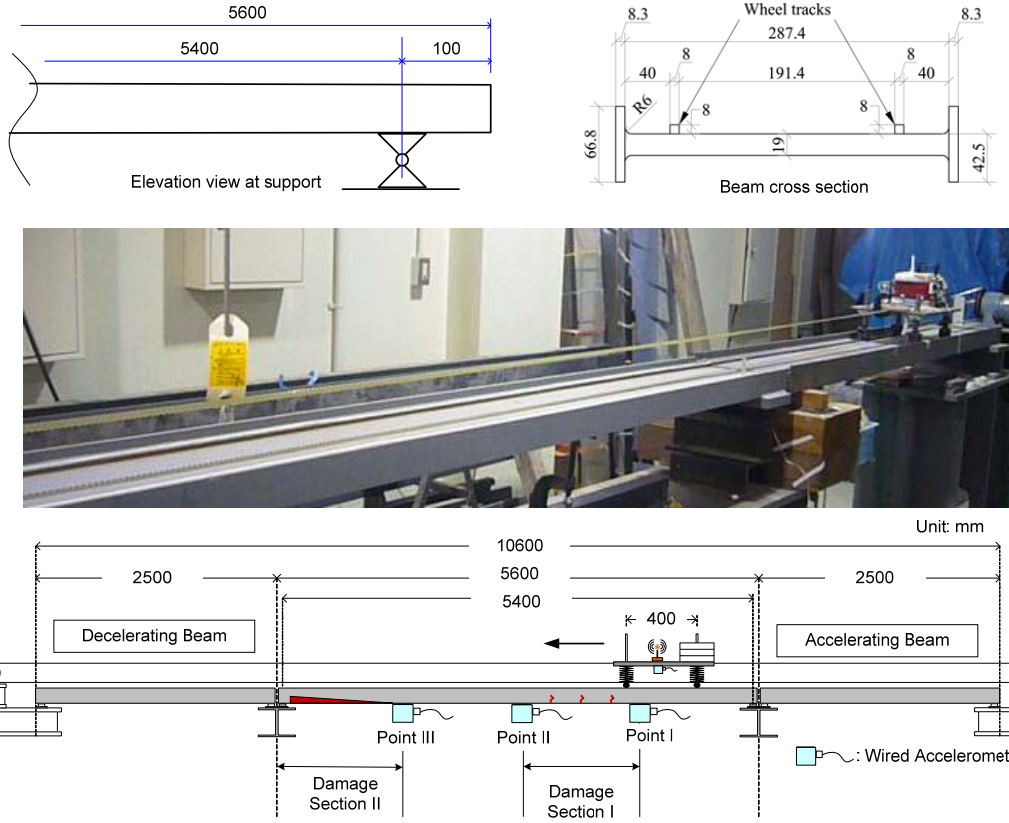


Fig. 1 Experimental girder and observation points

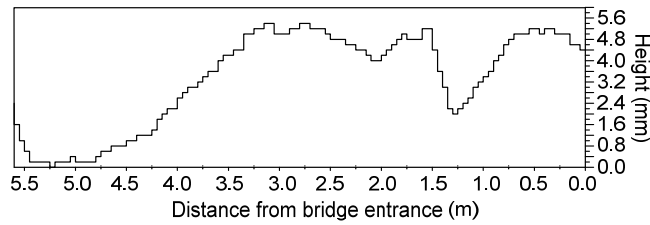


Fig. 2 Roadway profile

The denominator of the transfer function is the characteristic equation of the dynamic system shown in Eq. (25).

$$z^n + a_1 z^{n-1} + a_2 z^{n-2} + \dots + a_{n-1} z + a_n = 0 \quad (25)$$

The frequency and damping constant of each mode can be estimated from the complex conjugate poles as (e.g., Inman (2008))

$$z_k = \exp(h_k \omega_k \pm j \omega_k \sqrt{1-h_k}) \quad (26)$$

Therein, h_k indicates the damping constant; ω_k is circular frequency of k -th mode of the system; and j represents the imaginary unit.



Fig. 3 Photo of damage sections

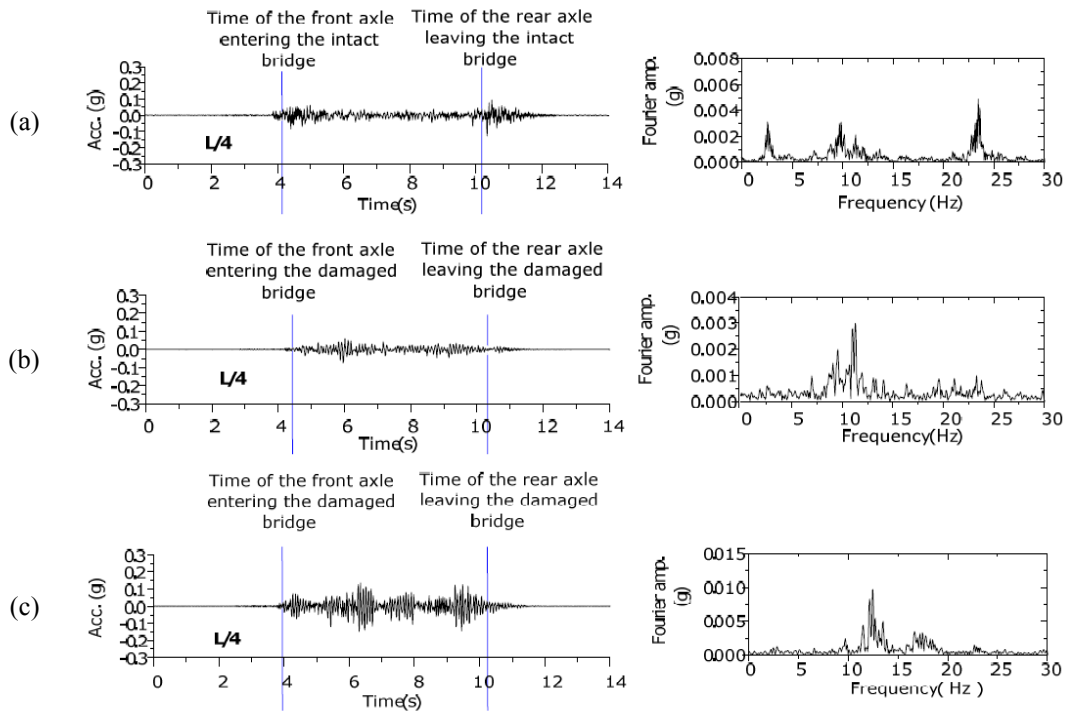


Fig. 4 Accelerations and Fourier spectra observed at point I: (a) Intact, (b) D1 and (c) D2

3. Laboratory experiment for traffic-induced vibration

A moving vehicle laboratory experiment was performed to investigate the validity of the proposed approach. The experimental setup is shown in Fig. 1. Roadway profiles shown in Fig. 2 were paved on the experiment girder. This study considers two different damages: one, called as damage section I, is that three saw cuts were applied both left and right sides of the flange between $L/4$ and $L/2$ of the model bridge; and the other, called as damage section II, is that a slanted cut-out up to 20.0 mm was applied both left and right sides of the flange between $3L/4$ and L of the experimental girder. Photos of damage sections are shown in Fig. 3. The bending rigidity of the

member decreased to around 89% comparing to the intact state due to damage scenario I. For the damage scenario II the bending rigidity decreased to 77% of the intact state. Regarding damage scenarios, the damage scenario of the bridge having damage section I was called as D1, and the damage scenario of bridge with both damage section I and damage section II was called as D2. Natural frequency estimated from free vibration of the intact state was 2.69 Hz; for damage scenario D1, 2.59 Hz; and for damage scenario D2, 2.54 Hz.

Three different vehicle models of which the natural frequency for the bounce motion is changeable using a different set of mass and spring were considered in the experiment. Three vehicles named as V1, V2 and V3 were used in the experiment. Natural frequencies for the bounce motion of the vehicle models were 2.93 Hz for V1 vehicle, 3.76 Hz for V2 vehicle and 3.03 Hz for V3 vehicle. Two different speeds of 0.93 m/s (hereafter, S1) and 1.63 m/s (hereafter, S2) were adopted to investigate the effect of the vehicle speed on damage identification results. Six traffic scenarios were considered: SCN1 of V1 vehicle traveling with speed of 0.93 m/s; SCN2 of V1 vehicle traveling with speed of 1.63 m/s; SCN3 of V2 vehicle traveling with speed of 0.93 m/s; SCN4 of V2 vehicle traveling with speed of 1.63 m/s; SCN5 of V3 vehicle traveling with speed of 0.93 m/s; and SCN6 of V3 vehicle traveling with speed of 1.63 m/s.

Three points at 1/4, 1/2 and 3/4 of the span length were observation points for acceleration responses as shown in Fig. 1. The sampling rate was 100 Hz. Examples of acceleration time histories of the experiment girder before and after applying damage are shown in Fig. 4 with the Fourier amplitude spectrum and each acceleration. The appearance of additional dominant

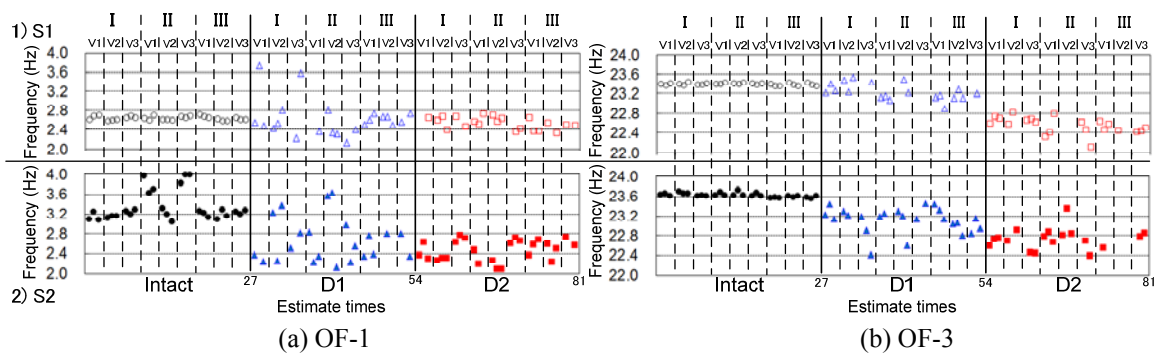


Fig. 5 System frequencies according to different damage patterns identified by SAR model

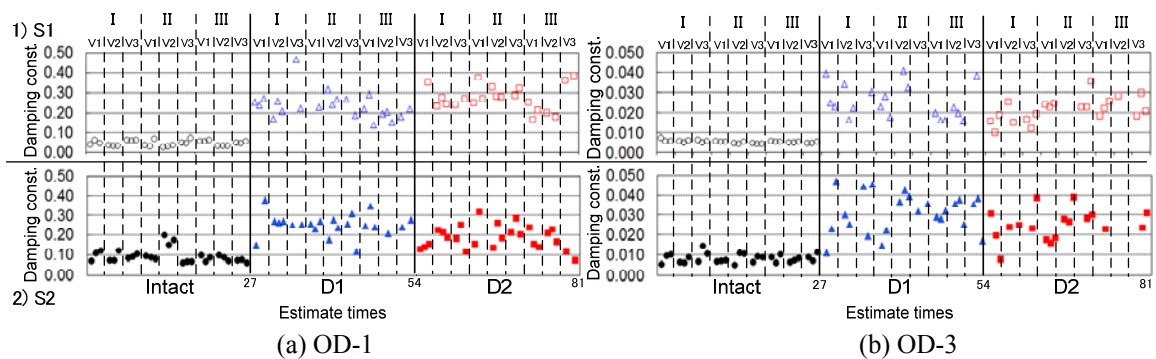


Fig. 6 System damping constants according to different damage patterns identified by SAR model

Table 1 Statistical feature of system frequencies identified by SAR model

		S1			S2		
		Intact	DI	D2	Intact	DI	D2
OF-1	Mean	2.63	2.62	2.53	3.34	2.67	2.46
	SD	0.041	0.369	0.123	0.290	0.444	0.207
	CV	0.015	0.141	0.049	0.087	0.166	0.084
OF-3	Mean	23.39	23.24	22.55	23.63	23.12	22.73
	SD	0.021	0.161	0.161	0.042	0.251	0.213
	CV	0.001	0.007	0.007	0.002	0.011	0.009

*OF-1: Observed Frequency for 1st mode, OF-3: Observed Frequency for 3rd mode
SD: Standard Deviation, CV: Coefficient of Variation

Table 2 Statistical feature of system damping constants identified by SAR model

		S1			S2		
		Intact	DI	D2	Intact	DI	D2
OD-1	Mean	0.0463	0.2371	0.2738	0.0944	0.2523	0.1863
	SD	0.0133	0.0662	0.0602	0.0331	0.0553	0.0571
	CV	0.288	0.279	0.220	0.351	0.219	0.306
OD-3	Mean	0.0054	0.0254	0.0214	0.0944	0.2523	0.1863
	SD	0.0006	0.0080	0.0058	0.0021	0.0097	0.0081
	CV	0.115	0.313	0.271	0.022	0.039	0.044

*OD-1: Observed Damping for 1st mode, OD-3: Observed Damping for 3rd mode

frequencies due to the damage in comparison with those of the intact girder was also observed. Dominant frequencies near 2.5 Hz and 23.4 Hz appearing in the intact bridge were weakened by damages.

4. System frequency and damping constant estimated by SAR model

System frequencies and damping constants estimated from the data of the six traffic scenarios were investigated. Fig. 5 shows summarized system frequencies; and Fig. 6 for system damping constants. AR order was $p=35$, which was not an optimal order but an empirical one. Statistical features of the identified system frequency are summarized in Table 1, and those for damping constant are summarized in Table 2. In Fig. 5, the first 27 plots indicate identified dominant frequencies estimated from the data of the intact girder, and those in Fig. 6 are estimated damping constants. On the contrary, the second 27 plots are those taken from the data of the damage scenario D1 and the third 27 plots are from damage scenario D2. I, II and III on the figures denote observation points. V1, V2 and V3 on the figures show vehicle type. Figs. 5(a) and (b) respectively show the first and third dominant frequencies, and those for damping constants are also shown in Figs. 6(a) and (b). Those second dominant frequencies and damping constants gave less clear pattern change between intact and damage girders than those for the first and third ones, and were omitted in this paper. Fig. 5 shows clear pattern change of identified dominant frequencies despite of their variations. An interesting point was the third dominant frequencies

revealed more apparent pattern changes according to the damage.

Usually the damping constants derived from eigenvalues of a system matrix are subject to appreciable error (Pappa and Ibrahim 1981). This study also observed greater variance of damping constants than that of the identified frequencies as shown in Fig. 6. However, despite of their appreciable error the pattern change of identified damping constants due to the damage was very apparent comparing to that of the dominant frequency shown in Fig. 5.

5. Structural diagnosis using parameter from AR coefficients

5.1 Indicator using autoregressive coefficients

This section focuses on diagnosis of bridges using a parameter taken from AR coefficients since a linear dynamic system can be idealized using the AR model as shown in Eq. (22)

$$y(k) = \sum_{i=1}^p a_i y(k-i) + e(k)$$

where, $y(k)$ denotes output of a system, a_i is the i -th order AR coefficient and $e(k)$ indicates the noise term.

The parameter from AR coefficients was adopted as a diagnosis indicator (DI), which is defined as

$$DI_j = \begin{cases} |a_1| & (j=1) \\ \frac{|a_1|}{\sqrt{\sum_{i=1}^j a_i^2}} & (j>1) \end{cases} \quad (27)$$

where, a_i denotes the i -th AR coefficient.

The AR process with the model order p in Eq. (22) can be expressed in the z -transform domain as shown in Eq. (24). The $H(z)$ in Eq. (24) is defined as AR polynomial of the model transfer function relating the input to output. The poles z_k in Eq. (26) are obtained by finding the roots of the AR coefficient polynomial in the denominator of $H(z)$. Since the coefficient of $H(z)$ are real, the roots must be real or complex conjugate pairs. The number of poles in z plane equals to the AR model order. Therefore z_k shown in Eq. (26) and AR coefficients have following relationships.

$$\begin{aligned} \sum_i z_i &= -a_1 \\ \sum_{i,j} z_i z_j &= a_2 \\ \sum_{i,j,k} z_i z_j z_k &= -a_3 \end{aligned} \quad (28)$$

Eqs. (26) and (28) show AR coefficients directly link to system frequencies and damping constant. Therefore, AR coefficient changes due to damage, and DI also changes due to damage. This is the theoretical background of AR coefficient for structural diagnosis. Another way to

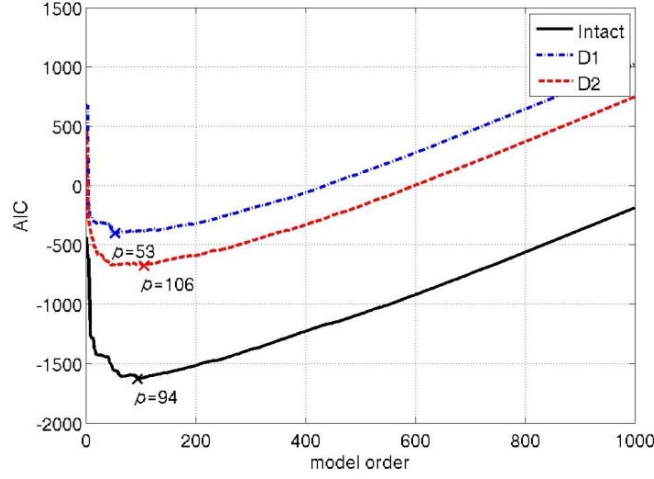


Fig. 7 AIC with respect to model order of SAR model (p =optimal AR order)

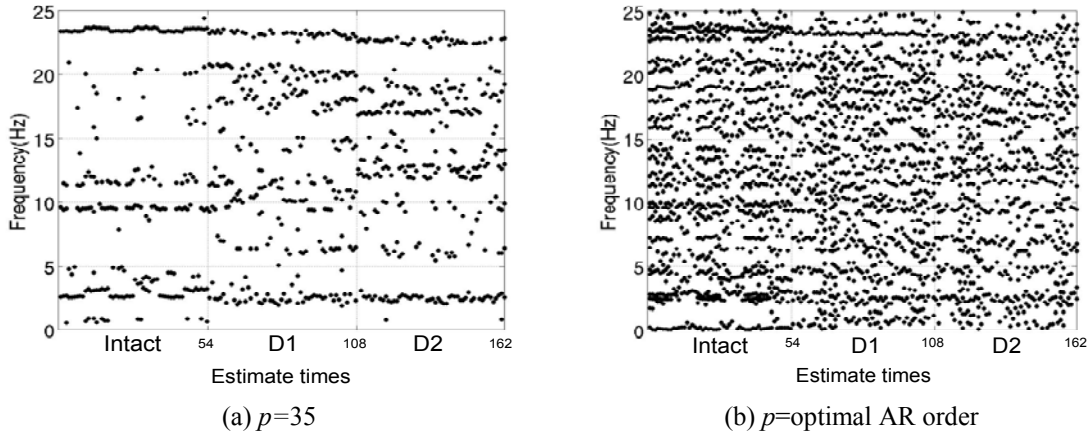


Fig. 8 Estimated Frequencies by SAR mode

explain the relationship between AR coefficient and circular frequency and damping constant is shown in Appendix A.

In this study, the optimal order of the AR model was selected by means of AIC (Akaike Information Criterion) shown in Eq. (29).

$$\text{AIC} = N \log(2\pi\hat{\sigma}_M^2) + 2(M + 1) + N \quad (29)$$

where N indicates the number of data; M , AR order; and $\hat{\sigma}_M^2$, mean square of M th prediction error. The AIC consists of two terms, the first term is a log-likelihood function and the second term is a penalty function for the number of the AR order. Fig. 7 shows behavior of order selection criteria by AIC. Fig. 8 show estimated result of system frequency: (a) $p=35$, (b) p =optimal AR order. Comparing Figs. 8(a) and (b) using optimal AR order for frequency identification gave both system and numerical frequencies. These numerical frequencies usually interfere to select system

frequencies. That was one reason of focusing on AR coefficient for structural diagnosis. Another interesting observation was that, as shown in Fig. 7, the AIC value at the optimal AR order was changed apparently due to damage. In other words AIC at the optimal AR order can be utilized as a damage-sensitive feature.

5.2. Sensitivity analysis

This study performed a sensitivity analysis to decide the most sensitive DI_j due to damage. The DI_j which is obtained by changing the order j from 1 to 6 is summarized in Fig. 9. The difference of DI_j between intact and damage bridges with respect to j were estimated as shown in Fig. 10: Fig. 10(a) for Intact vs. D1; and Fig. 10(b) for Intact vs. D2. Fig. 10 clearly indicates that difference of DI between intact and damage bridges is the most apparent when j takes 3. Therefore this study adopted DI_3 as a damage sensitive feature.

5.3. Singlevariate AR model

A preliminary study by authors shows that the DI is affected by observation points and vehicle speeds (Kim *et al.* 2011). So this study examined change of the DI according to damage, observation points and vehicle speeds as shown in Fig. 11.

For DI observed at point I and point III under vehicle speed of S1, it is hard to read a clear change of the DI due to damage. On the other hand, the DI observed at point II clearly shows change due to damage. For the vehicle speed of S2 which was faster than S1, pattern change of the DI due to damage was observed at all observation points due to damage.

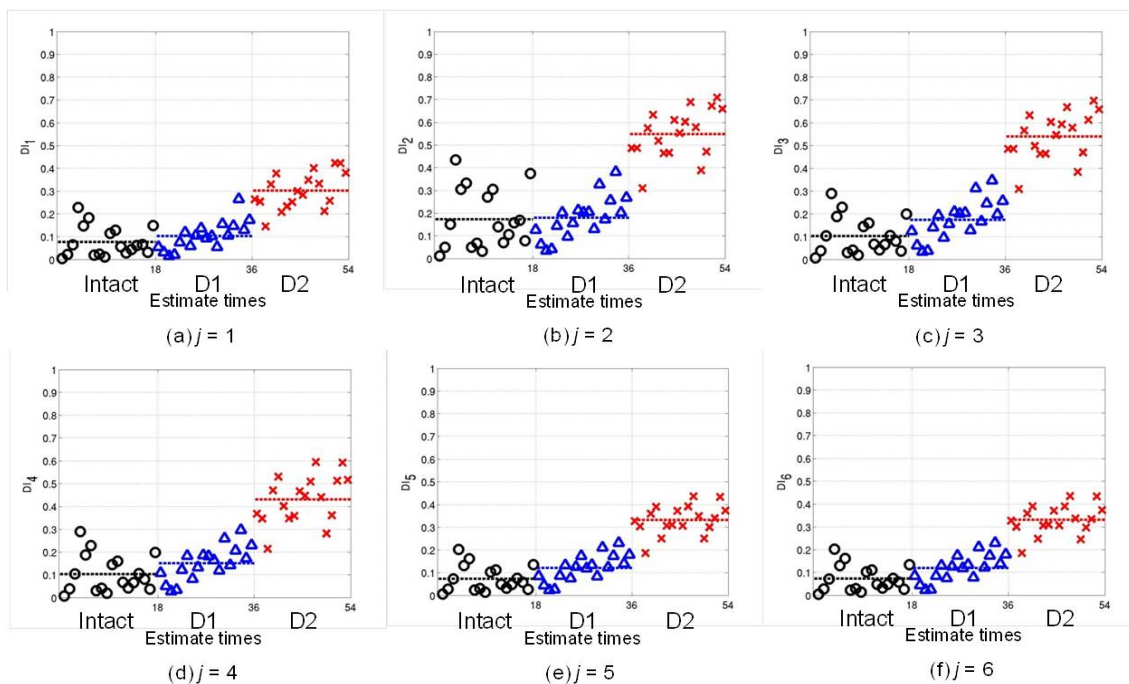


Fig. 9 DI with respect to the order of AR coefficient of SAR model considering in denominator of Eq. (27)

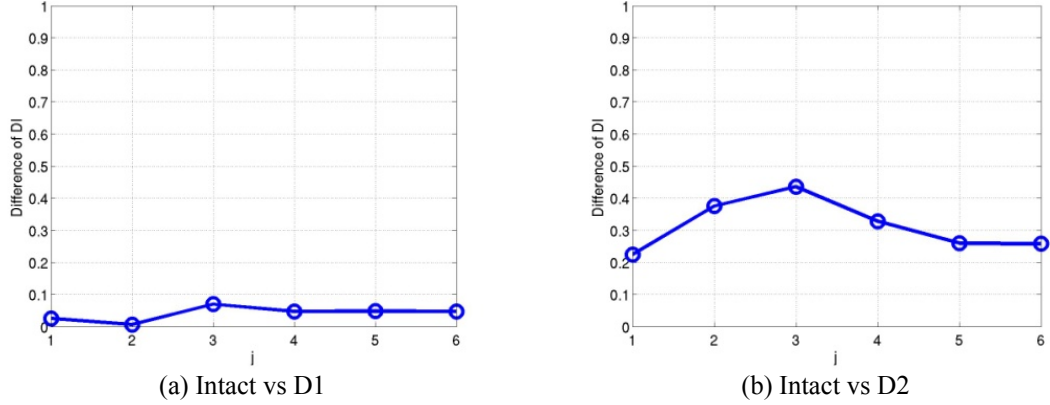


Fig. 10 Difference of DI with respect to the order of AR coefficient of SAR model considering in denominator of Eq. (27)

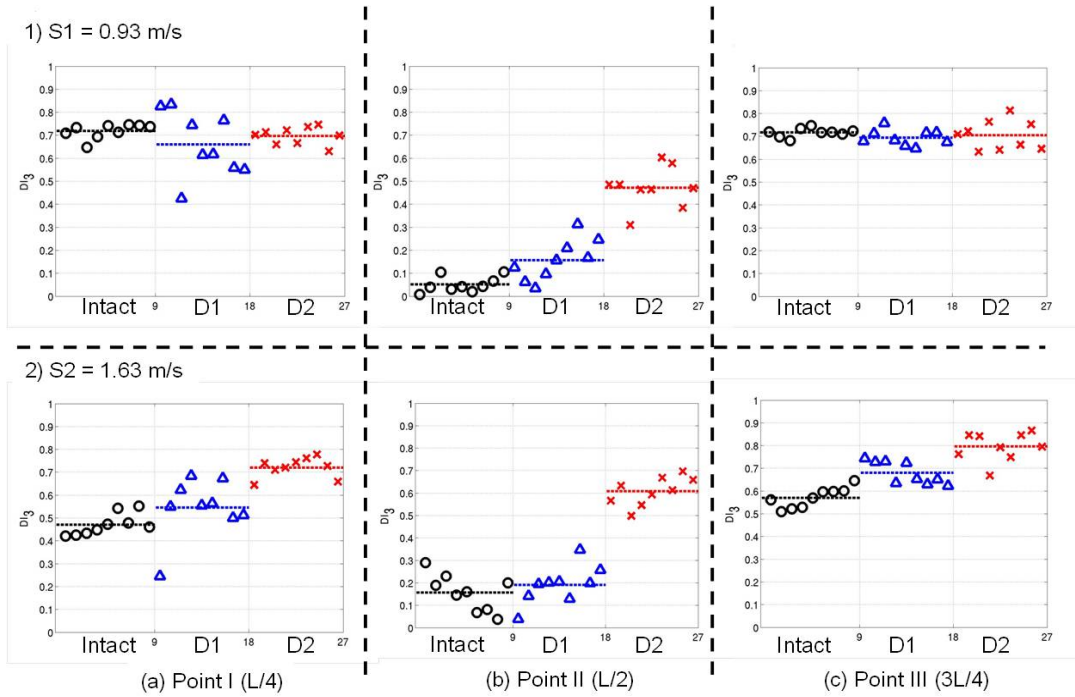


Fig. 11 Variation of DI_3 identified by SAR model according to different damage patterns, speeds and observation points

5.4. Multivariate AR model

A parameter from the MAR model shown in Eq. (30) is also used to derive a damage sensitive feature.

$$\mathbf{y}(k) = \sum_{i=1}^u \mathbf{G}_i \mathbf{y}(k-i) + \mathbf{e}(k) \quad (30)$$

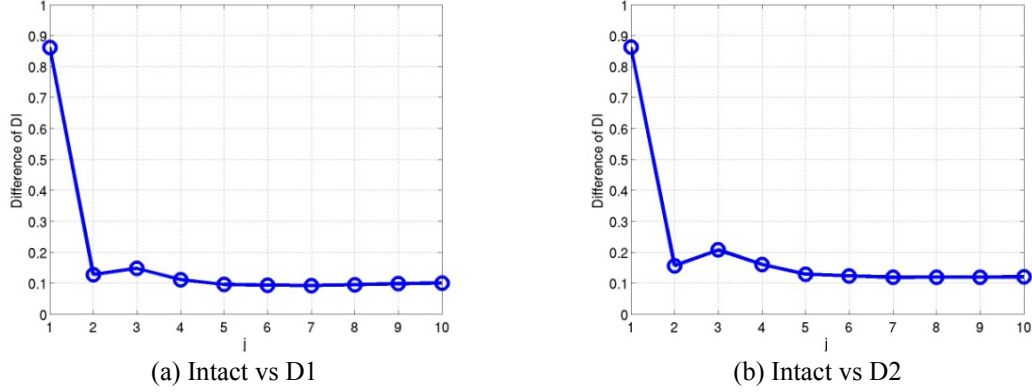


Fig. 12 Difference of DI identified by MAR model with respect to the order of coefficient of Eq. (32(b))

where, $\mathbf{y}(k)$ denotes outputs of a system, \mathbf{G}_i is AR coefficients matrices in the system matrix $\hat{\mathbf{A}}$ and $\mathbf{e}(k)$ is the noise term. The system matrix $\hat{\mathbf{A}}$ is shown in Eq. (31).

$$\hat{\mathbf{A}} = \begin{bmatrix} \mathbf{0} & \mathbf{I} & \mathbf{0} & \cdots & \mathbf{0} \\ \mathbf{0} & \mathbf{0} & \mathbf{I} & \cdots & \mathbf{0} \\ \vdots & & & \ddots & \vdots \\ \mathbf{0} & \mathbf{0} & \mathbf{0} & & \mathbf{I} \\ -\mathbf{G}_p & -\mathbf{G}_{p-1} & -\mathbf{G}_{p-2} & \cdots & -\mathbf{G}_1 \end{bmatrix} \quad (31)$$

Details of the process are obtainable from existing study by Kim *et al.* 2010. The characteristic equation of the system matrix $\hat{\mathbf{A}}$ is writable as Eq. (32).

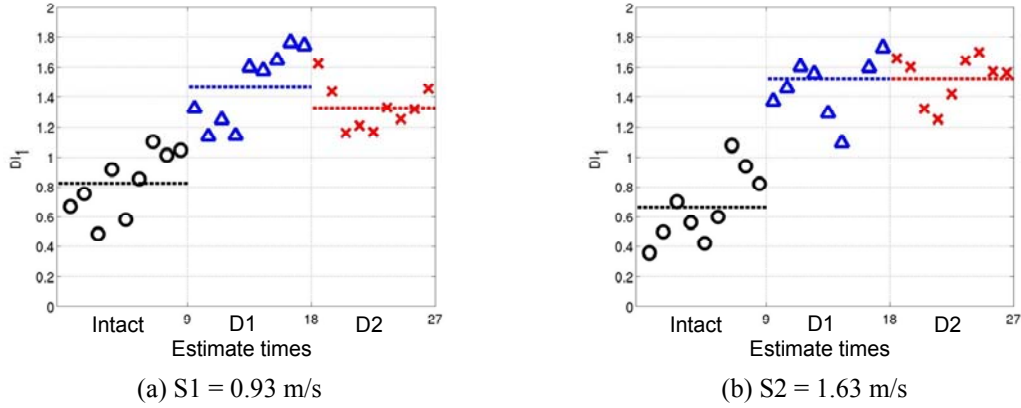
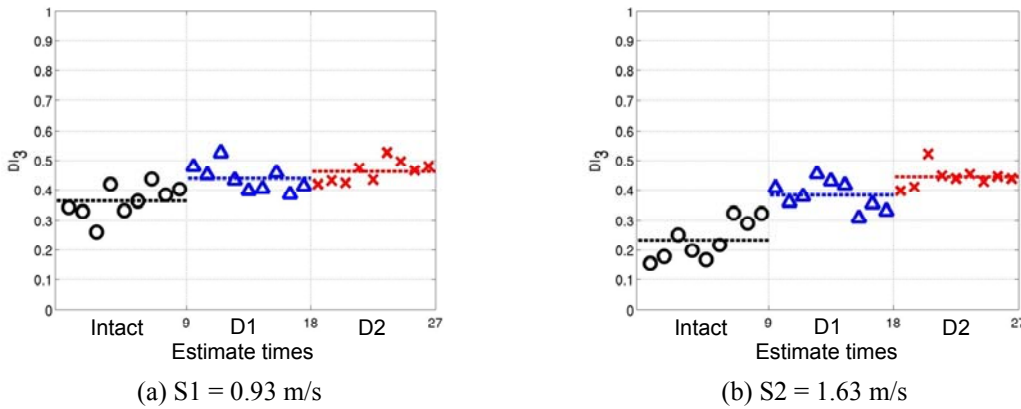
$$\det(\hat{\mathbf{A}} - \lambda \mathbf{I}) = 0 \quad (32a)$$

$$\lambda^n + c_1 \lambda^{n-1} + c_2 \lambda^{n-2} + \cdots + c_n = 0 \quad (32b)$$

where, λ indicates eigenvalues of the system matrix and \mathbf{I} is the unit matrix. The relationship between the coefficient c_i and eigenvalues of system matrix λ can be also written as

$$\begin{aligned} \sum_i \lambda_i &= -c_1 \\ \sum_{i,j} \lambda_i \lambda_j &= c_2 \\ \sum_{i,j,k} \lambda_i \lambda_j \lambda_k &= -c_3 \end{aligned} \quad (33)$$

When the structure is damaged, the system matrix change due to damage and eigenvalue of the system matrix also change due to damage. So, Eq. (33) indicates that the coefficient c_i changes due to damage. The coefficient c_i of Eq. (32(b)) has same meaning with the AR coefficient of Eq. (25). As is the case with SAR model, this study performed a sensitive analysis according to Eq. (27). Fig. 12 shows the result of sensitive analysis. It is shown that when j takes 1, DI_j is the most sensitive parameter due to damage. Therefore this study adopted DI_1 , which considers first order

Fig. 13 Variation of DI_1 identified by MAR model according to different damage patterns and speedsFig. 14 Variation of DI_3 identified by MAR model according to different damage patterns and speeds

coefficient of Eq. (32(b)), as a damage sensitive feature.

Fig. 13 shows the plots of DI estimated using the MAR model according to bridge's health conditions, which also demonstrates pattern change of DI due to damage. Change of DI also became clearer under the moving vehicle of higher speed ($S2$) than under the vehicle of lower speed ($S1$).

For reference, when j takes 3 which is similar with the case of SAR model, plots of DI_3 according to bridge's health conditions are shown in Fig. 14. Of course DI_1 gives more clear changes due to damages than DI_3 .

6. Conclusions

This paper investigated the feasibility of BHM using traffic-induced vibration measurements of a model bridge through a laboratory experiment. This study considered AR coefficients as an early indicator of abnormalities of bridges. The summarized results are as follows.

The DI value taken from traffic-induced vibration data provided information to make a decision

on diagnosis of short span bridges. The pattern of DI estimated using the data in higher vehicle speed gave better chance to make a decision on bridge diagnosis. Another interesting result was that the parameter from the data measured at the span center was the most sensitive to damage for the SAR model. Both SAR and MAR models showed similar results. However the MAR model required longer computation time to find an optimal MAR model than the SAR model. An interesting observation was that the AIC at the optimal AR order showed apparent change due to damage. The feasibility of AIC as a damage indicator needs a comprehensive, which is the next step for this study.

References

- Deraemaeker, A., Reynders, E., De Roeck, G. and Kullaa, J. (2007), "Vibration-based structural health monitoring using output-only measurements under changing environment", *Mech. Syst. Signal Pr.*, **22**(1), 34-56.
- Dilena, M. and Morassi, A. (2011), "Dynamic testing of damaged bridge", *Mech. Syst. Signal Pr.*, **25**(5), 1485-1507.
- Doebbling, S.W., Farrar, C.R., Prime, M.B. and Shevitz, D.W. (1996), *Damage identification and health monitoring of structural and mechanical systems from changes in their vibration characteristics: A literature review*, Los Alamos National Laboratory Report LA-3070-MS.
- Gersch, W., Nielsen, N.N. and Akaike, H. (1973), "Maximum likelihood estimation of structural parameters from random vibration data", *J. Sound Vib.*, **31**(3), 295-308.
- He, X. and De Roeck, G. (1997), "System identification of mechanical structures by a high-order multivariate autoregressive model", *Comput. Struct.*, **64**(1-4), 341-351.
- Hoshiya, M. and Saito, E. (1984), "Structural identification by extended Kalman filter", *J. Eng. Mech.-ASCE*, **110**(12), 1757-1770.
- Inman, D.J. (2008), *Engineering vibration*, 3rd Ed., Upper Saddle River, N.J., PTR Prentice Hall.
- Kim, C.W., Kawatani, M. and Kim, K.B. (2005), "Three-dimensional dynamic analysis for bridge-vehicle interaction with roadway roughness", *Comput. Struct.*, **83**(19-20), 1627-1645.
- Kim, C.W. and Kawatani, M. (2008), "Pseudo-static approach for damage identification of bridges based on coupling vibration with a moving vehicle", *Struct. Infrastruct. E.*, **4**(5), 371-379.
- Kim, C.W. and Kawatani, M. and Hao, J. (2010), "Model parameter identification of short span bridges under a moving vehicle by means of multivariate AR model", *Struct. Infrastruct. E.*, **8**(5), 459-472.
- Kim, C.W., Isemoto, R., Kawatani, M. and Sugiura, K. (2011), "Structural diagnosis of bridge using output-only vibration in moving vehicle laboratory experiment", *JSCE J. Appl. Mech.* (In Japanese)
- Ljung, L. (1999), *System identification-Theory for the user*, 2nd Ed., PTR Prentice Hall, Upper Saddle River, M.J.
- Nair, K.K., Kiremidjian, A.S. and Law, K.H. (2006), "Time series-based damage detection and localization algorithm with application to the ASCE benchmark structure", *J. Sound Vib.*, **291**(1-2), 349-368.
- Pappa, R.S. and Ibrahim, S.R. (1981), "A parametric study of the Ibrahim time domain modal identification algorithm", *Shock Vib.*, **51**(3), 43-72.
- Peeters, B. and De Roeck, G. (2001), "One-year monitoring of the Z24-Bridge: environmental effects versus damage events", *Earthq. Eng. Struct. D.*, **30**(2).
- Shinozuka, M., Yun C.B. and Imai, H. (1982), "Identification of linear structural dynamic systems", *J. Eng. Mech. - ASCE*, **108**(6), 1371-1390.
- Wang, Z. and Fang, T. (1986), "A time-domain method for identifying model parameters", *J. Appl. Mech.-ASME*, **53**(3), 28-32.
- Zhang, Q.W. (2007), "Statistical damage identification for bridges using ambient vibration data", *Comput. Struct.*, **85**(7-8), 476-485.

Appendix A

Dynamic equation of motion for a system is writable as Eqs. (A1) and (A2).

$$m_c \ddot{y}(t) + c_c \dot{y}(t) + k_c y(t) = 0 \quad (\text{A1})$$

$$\ddot{y}(t) + 2h\omega_0 \dot{y}(t) + \omega_0^2 y(t) = 0 \quad (\text{A2})$$

where, h denotes damping constant of the system, and ω_0 is circular frequency.

A general solution is

$$y(t) = G e^{-\lambda t} \sin(\omega t + \varphi) \quad (\text{A3})$$

$$\omega = \omega_0 \sqrt{1 - h^2} \quad (\text{A4})$$

$$\lambda = \omega_0 h \quad (\text{A5})$$

where, G is unknown constant and φ indicates unknown phase angle.

The time history of a dynamic system shows in Eq. (A2) can be modeled by the AR process as

$$y_n = a_1 y_{n-1} + a_2 y_{n-2} + \dots + a_n y_{n-m} + \dots \quad (\text{A6})$$

Using Eq. (A3) the dynamic response y_n is rewritable as

$$y_n = G e^{-\lambda t_n} \sin(\omega t_n + \varphi) \quad (\text{A7})$$

$$\begin{aligned} y_{n-k} &= G e^{-\lambda(t_n - k\Delta t)} \sin\{\omega(t_n - k\Delta t) + \varphi\} \\ &= G e^{\lambda k\Delta t} e^{-\lambda t_n} \sin\{\omega(t_n - k\Delta t) + \varphi\} \\ &= G e^{\lambda k\Delta t} e^{-\lambda t_n} \{\sin(\omega t_n + \varphi) \cos(\omega k\Delta t) - \cos(\omega t_n + \varphi) \sin(\omega k\Delta t)\} \end{aligned} \quad (\text{A8})$$

To simplify the problem, we consider the AR process with the 2nd order.

$$y_{n-1} = G e^{\lambda \Delta t} e^{-\lambda t_n} \{\sin(\omega t_n + \varphi) \cos(\omega \Delta t) - \cos(\omega t_n + \varphi) \sin(\omega \Delta t)\} \quad (\text{A9})$$

$$\begin{aligned} y_{n-2} &= G e^{\lambda 2\Delta t} e^{-\lambda t_n} \{\sin(\omega t_n + \varphi) \cos(\omega 2\Delta t) - \cos(\omega t_n + \varphi) \sin(\omega 2\Delta t)\} \\ &= G e^{\lambda 2\Delta t} e^{-\lambda t_n} \{\sin(\omega t_n + \varphi) (1 - 2\sin^2(\omega \Delta t)) - \cos(\omega t_n + \varphi) (2\sin(\omega \Delta t) \cos(\omega \Delta t))\} \end{aligned} \quad (\text{A10})$$

From Eq. (A7), we obtain the following

$$G = \frac{y_n}{e^{-\lambda t_n} \sin(\omega t_n + \varphi)} \quad (\text{A11})$$

By substituting Eq. (A11) into Eq. (A9), we can obtain following equation.

$$\begin{aligned} y_{n-1} &= y_n e^{\lambda \Delta t} \left\{ \cos(\omega \Delta t) - \frac{\cos(\omega t_n + \varphi)}{\sin(\omega t_n + \varphi)} \sin(\omega \Delta t) \right\} \\ - \frac{\cos(\omega t_n + \varphi)}{\sin(\omega t_n + \varphi)} \sin(\omega \Delta t) &= \frac{y_{n-1}}{y_n} e^{-\lambda \Delta t} - \cos(\omega \Delta t) \end{aligned} \quad (\text{A12})$$

Substituting Eq. (A11) into Eq. (A10) gives

$$\begin{aligned}
 y_{n-2} &= y_n e^{\lambda 2\Delta t} \left\{ (1 - 2 \sin^2(\omega \Delta t)) - \frac{\cos(\omega t_n + \varphi)}{\sin(\omega t_n + \varphi)} (2 \sin(\omega \Delta t) \cos(\omega \Delta t)) \right\} \\
 &= y_n e^{\lambda 2\Delta t} \left\{ (1 - 2 \sin^2(\omega \Delta t)) + \left(\frac{y_{n-1}}{y_n} e^{-\lambda \Delta t} - \cos(\omega \Delta t) \right) (2 \cos(\omega \Delta t)) \right\} \quad (A13)
 \end{aligned}$$

$$\begin{aligned}
 &= y_n e^{\lambda 2\Delta t} \left\{ (1 - 2 \sin^2(\omega \Delta t)) + 2 \frac{y_{n-1}}{y_n} e^{-\lambda \Delta t} \cos(\omega \Delta t) - 2 \cos^2(\omega \Delta t) \right\} \\
 &= y_n e^{\lambda 2\Delta t} \left\{ 2 \frac{y_{n-1}}{y_n} e^{-\lambda \Delta t} \cos(\omega \Delta t) - 1 \right\} \quad (A14) \\
 &= 2 e^{\lambda \Delta t} \cos(\omega \Delta t) y_{n-1} - e^{\lambda 2\Delta t} y_n \\
 e^{\lambda 2\Delta t} y_n &= 2 e^{\lambda \Delta t} \cos(\omega \Delta t) y_{n-1} - y_{n-2}
 \end{aligned}$$

Eq. (A14) is rewritable in general formation as

$$y_n = 2 e^{-\lambda \Delta t} \cos(\omega \Delta t) y_{n-1} - e^{-\lambda 2\Delta t} y_{n-2} \quad (A15)$$

Comparing Eq. (A15) with Eq. (A6) of 2nd order

$$a_1 = 2 e^{-\lambda \Delta t} \cos(\omega \Delta t) y_{n-1} \quad (A16)$$

$$a_2 = -e^{-\lambda 2\Delta t} \quad (A17)$$

From Eqs. (A16) and (A17), we can obtain following relationship.

$$\lambda = \frac{\ln(-a_2)}{2\Delta t} \quad (A18)$$

$$\omega = \frac{1}{\Delta t} \cos^{-1} \left(\frac{a_1}{2\sqrt{-a_2}} \right) \quad (A19)$$

It also shows that AR coefficients directly link with dynamic characteristic of systems.